16TH EUROPEAN CONFERENCE ON EARTHQUAKE ENGINEERING THESSALONIKI 18 - 21 JUNE 2018

EXPERIMENTAL STUDY ON SEISMICALLY ISOLATED STRUCTURES: CAN THE ISOLATED SUPERSTRUCTURE YIELD?

Anastasios TSIAVOS[1], David SCHLATTER[2], Bozidar STOJADINOVIC[3]

ABSTRACT

Seismically isolated structures are designed elastically, according to the current American and European code provisions. The goal of this study is to demonstrate the necessity of such elastic design of seismically isolated structures through the experimental and analytical investigation of their inelastic response. This inelastic response can be triggered when seismically isolated structures are subjected to events of higher seismic hazard than the design hazard level.

The experimental investigation of the inelastic behavior of seismically isolated structures is performed using a reduced-scale base-isolated steel specimen subjected to strong ground motion records. These ground motions are applied using the shaking table of the IBK Structural Testing laboratory of ETH Zurich. The inelastic behavior of the specimen is concentrated in a pair of steel coupons that can be easily replaced. Four friction pendulum bearings are used for seismic isolation of the structure.

The analytical investigation of the inelastic response of seismically isolated structures is performed via a two-degree-of-freedom model of a base-isolated structure. The bilinear hysteretic behavior of the structure and the isolator is simulated using Bouc-Wen models. The response of the modelled structure to a large number of strong ground motion records is determined using Matlab and Opensees.

The analytically investigated inelastic behavior of seismically isolated structures is compared to the experimentally observed behavior. A relation between the strength reduction factor and the displacement ductility demand of these structures is presented based on the results of the analytical and experimental investigation. A parametric analysis is performed to determine the effects of isolator and superstructure design parameters on the response. The proposed strength-ductility relation lays the foundation for an effective seismic evaluation of existing seismically isolated structures and increases the understanding of the inelastic behavior of these structures.

Keywords: Experimental investigation of base-isolated structures; Inelastic behavior of base-isolated structures; Friction-pendulum bearings

1. INTRODUCTION

The response of seismic isolation bearings has been investigated analytically (Constantinou et al. 1990) and experimentally (Becker et al. 2012, Lignos 2012) towards the determination of the behavior of seismically isolated structures subjected to different types of ground motion excitation (Shi et al. 2014). Whittaker et al. (2017) summarized the applications of seismic isolation for buildings and bridges in the modern era. In most of these studies, the isolated superstructures are designed to remain in the elastic behavior range when subjected to the design-level ground motions.

The dynamics of the inelastic response of seismically isolated superstructures are less well understood. Such inelastic response can manifest itself in two cases. First, the design forces of the superstructure could be exceeded due to, for example, a ground motion stronger than the design ground motion level, or due to construction of a superstructure that is weaker than the designed one. Second, inelastic design of base-isolated structures for design-basis ground motions reduces the cost of the construction of the superstructure and thereby offsets the cost of the seismic isolation system.

[1]Postdoctoral Researcher, ETH Zurich, Stefano-Franscini-Platz 5, 8093, Zurich, tsiavos@ibk.baug.ethz.ch
[2]Student, ETH Zurich, Stefano-Franscini-Platz 5, 8093, Zurich, daschlatter@gmail.com
[3]Professor, ETH Zurich, Stefano-Franscini-Platz 5, 8093 Zurich, stojadinovic@ibk.baug.ethz.ch

The inelastic response of base-isolated structures has been studied by Constantinou and Quarshie (1998), Sollogoub (2003), Kikuchi et al. (2008), Thiravechyan et al. (2012) and Cardone et al. (2013). The researchers agreed that allowing seismically isolated superstructures to yield requires careful consideration. Tsiavos et al. (2013a, 2013b, 2017) and Vassiliou et al. (2013) concluded that designing typical seismically isolated superstructures to behave elastically, as prescribed by current seismic design codes, is not overly conservative but a necessity that emerges from the fundamental dynamics of such structures.

2. DYNAMIC MODELLING

Naeim and Kelly (1997) investigated the dynamics of a base-isolated structure analytically using a two-degree-of-freedom (2DOF) model similar to the one presented in Fig. 1. The system consisting of the isolation bearings and the isolation base is defined as isolation system. The structure above the isolation system is defined as the isolated superstructure. The mass of the isolated superstructure is denoted as m_s and the mass of the base above the isolation system is denoted as m_b. The stiffness and damping k_s and c_s refer to the superstructure, while k_b and c_b refer to the base. Horizontal displacement u_s is the relative displacement of the superstructure with respect to the base and u_b is the horizontal displacement of the isolation bearings with respect to the ground. The ground displacement is denoted as u_g. Bilinear hysteretic models have been chosen to simulate the hysteretic behavior of the isolated superstructure and the isolation system, similar to the models used by Mavronikola and Komodromos (2014) and Katsanos and Sextos (2015).

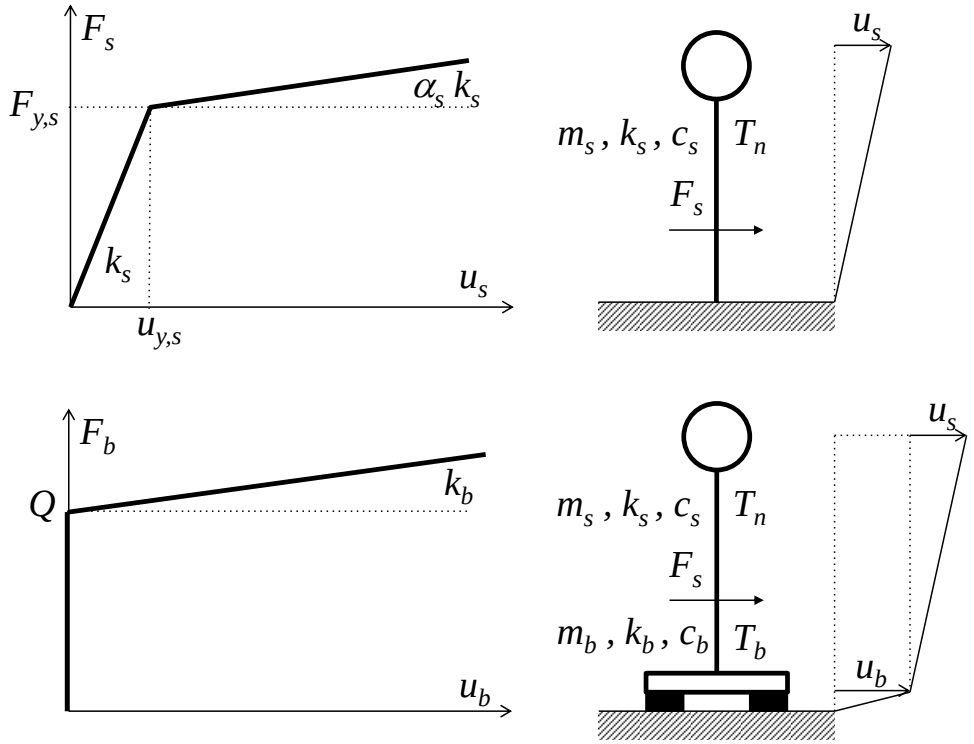

Fig. 1. Parameters of the SDOF model of a fixed-base structure and of a 2-DOF model of a base-isolated structure.

The notation used to describe the inelastic response of fixed-base single-degree-of-freedom (SDOF) structures is adopted as follows. The vibration period of the SDOF system is T_n. The displacement ductility ratio μ is defined as:

$$\mu = \frac{u_{m,s}}{u_{y,s}} \tag{1}$$

where $u_{m,s}$ and $u_{y,s}$ denote the maximum inelastic displacement and the yield displacement of the SDOF system, respectively. The strength reduction factor R_y is the ratio of the minimum strength required to maintain the SDOF system response in the elastic range, $F_{el,s}$ to the SDOF system yield strength $F_{y,s}$:

$$R_y = \frac{F_{el,s}}{F_{y,s}} \tag{2}$$

The following quantities are defined for the 2-DOF model of the base-isolated structure:

1. Period and cyclic frequency of the isolated superstructure:

$$T_n = 2\pi\sqrt{\frac{m_s}{k_s}}\ ,\ \omega_n = \sqrt{\frac{k_s}{m_s}} \tag{3}$$

2a. Isolation period and cyclic frequency:

$$T_b = 2\pi\sqrt{\frac{m_s + m_b}{k_b}},\ \omega_b = \sqrt{\frac{k_b}{m_s + m_b}} \tag{4}$$

2b. Effective isolation period and cyclic frequency:

$$T_{eff} = 2\pi\sqrt{\frac{m_s + m_b}{k_{eff}}},\ \omega_{eff} = \sqrt{\frac{k_{eff}}{m_s + m_b}} \tag{5}$$

3. Non-hysteretic structural and isolation system damping ratios:

$$\xi_s = \frac{c_s}{2m_s\omega_s},\qquad \xi_b = \frac{c_b}{2\left(m_s + m_b\right)\omega_b} \tag{6}$$

4. Mass ratio:

$$\gamma_m = \frac{m_s}{m_s + m_b} \tag{7}$$

3. EXPERIMENTAL INVESTIGATION

3.1 Design of the experimental setup

The goal of the design is to obtain a seismically isolated structure with the following design requirements:
1. Activation of the seismic isolation system before yielding of the isolated superstructure.
2. Concentration of the inelastic behavior of the isolated superstructure in a specifically designed element, which can be easily constructed and replaced.
3. The fixed-base period T_n of the superstructure shall resemble the one of a short, couple-of-story building: 0.3s $<T_n<$0.5s
4. The period of the isolated structure shall be roughly five times greater than the one of the fixed base structure ($T_B > 5T_n$), to widely separate the already orthogonal structural and seismic isolation vibration modes.
5. The total mass of the system shall not exceed 1000kg.

As shown in Fig. 2, the constructed structure is a seismically isolated cantilever structure with a lumped mass m_s attached on the top. The cantilever structural system consists of two vertical steel columns,

connected horizontally with 7 stiffening steel beams that guarantee the in-plane behavior of the system under shaking table excitation. The steel beams are anchored to a bottom plate. This plate is supported by two hinge elements (Fig. 2, 3) that allow the rotation of the plate in the plane of the excitation and two steel coupons (Fig. 3) that restrain this rotation. These four elements are anchored to another plate, which is supported by the base plate of the isolation system with mass m_b. Both plates above the base plate are equipped with small gaps that allow for the easy replacement of the steel coupons in case of damage. The isolation system consists of 4 friction pendulum bearings, which are distributed symmetrically on the shaking table. Table 1 shows the dimensions of the components of the isolated structure.

Figure 2. Constructed isolated structure in the ETH laboratory

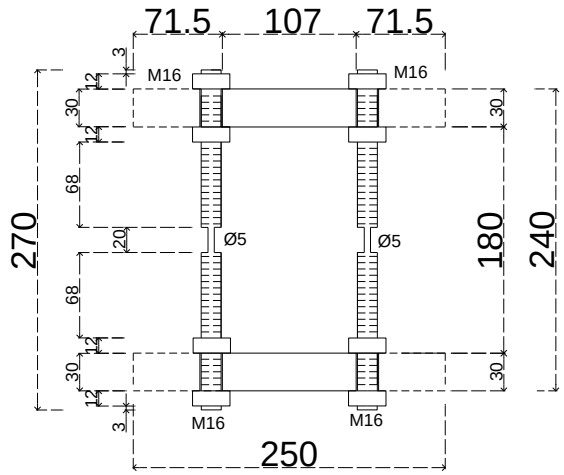

Figure 3. Elevation view of the 2 steel coupons (Dimensions in mm, Steel quality S275)

Table 1. Structural components of the designed isolated structure

Part	Material	Quality	Length (mm)	Width (mm)	Thickness (mm)	Height (mm)	Weight (kg)	Radius (mm)
1. Top mass	Steel	S235	750	150	170	-	250	-
2. Column-Superstructure	Steel	S235	1345	2100	10	1600	8	-
3. Base plate	Steel	S235	2.5	2.5	30	-	665	-
4. Bearing	Steel	S235	-	-	-	-	75	1500
5. Shaking Table	Steel	S235	1000	2000	-	-	-	-

The isolators are made by MAGEBA SA as the small version of their RESTON Pendulum Type Mono isolator. The fixed-base period of the constructed structure is T_n=0.52s, as measured in a free vibration test. The post-yielding isolation period T_b=2.3s was determined using a sine sweep shaking table excitation. The measured value of the yield strength of the isolation system is Q=520N. The differences stem from the inevitable discrepancies between the nominal and the actual mechanical properties of the components. The mass ratio of the constructed structure is γ_m=0.2. Two different diameters have been used for the reduced-diameter middle part of the steel coupons shown in Fig. 3, one of $D_{sc,2}$=4mm and one of $D_{sc,2}$=5mm.

3.2 Ground motion response data

The isolated structure shown in Fig. 2 was excited by 4 different ground motion excitations taken from the PEER Center ground motion database (2010), as shown in Table 2. These motions were chosen to simulate a wide variety of ground motion types, magnitudes and distances from the epicenter.

Table 2: Ground motion ensemble

Earthquake	Station	Record	Scale factor of the original motion (%)	PGA of the scaled motion (g)
San Fernando 1971	279 Pacoima Dam	PCD164	35	0.43
Tabas 1978	9101 Tabas	TAB-LN	32.5	0.27
Coalinga 1983	1651 Transmitter Hill	D-TSM270	100	0.71
Northridge 1994	USGS/VA 637 LA-Sepulveda VA Hospital	0637-270	75	0.56

3.2.1 Response to the 32.5% 1978 Tabas ground motion excitation

The scaled-down Tabas ground motion acceleration record is shown in Fig. 4. The measured relative displacement response time history of the top mass of the superstructure with respect to the base plate and the relative displacement time history of the base plate with respect to the shaking table are shown in Fig. 5. The elastic force in the superstructure was not measured but was computed analytically for each ground motion excitation using the experimentally determined properties of the isolators and the isolated superstructure.

The hysteretic force-displacement loop for the superstructure is shown in Fig. 6. The observed loop indicates that the isolated superstructure manifested significant inelastic behavior during this motion. The maximum measured displacement of the superstructure for this motion was 23.2 mm. The strength reduction factor R_y=1.7. Divided by the yield displacement of the superstructure, this maximum displacement leads to a displacement ductility μ=1.7. The maximum displacement of the isolation system was 72mm. The residual displacement of the isolation system due to this motion was 11mm.

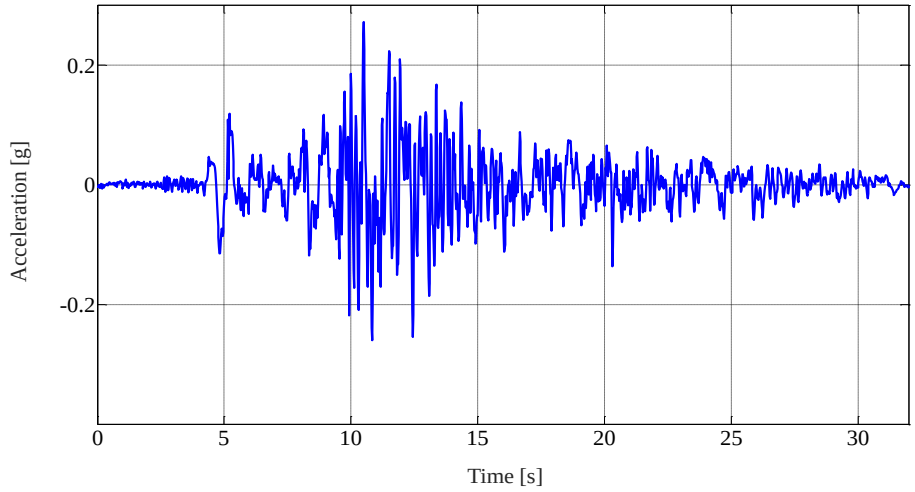

Fig. 4. 32.5%-scaled 1978 Tabas ground motion excitation

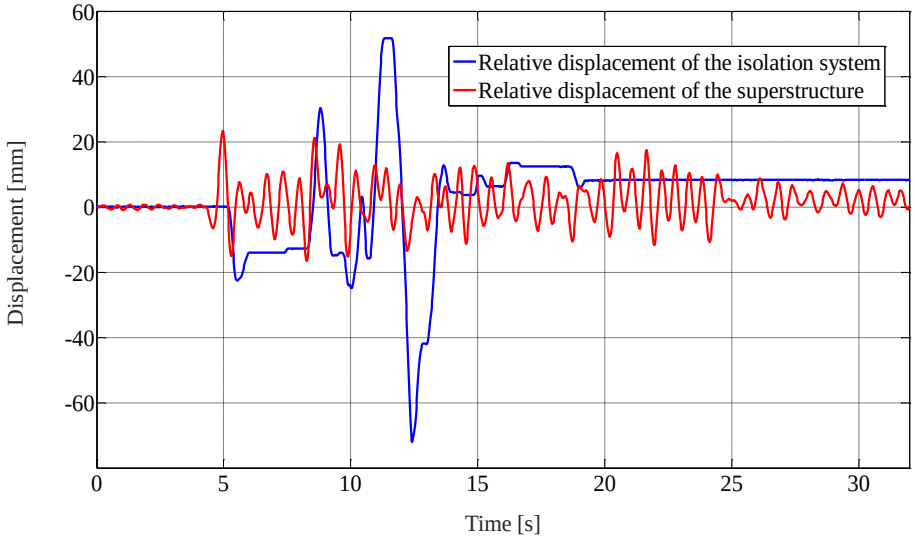

Fig. 5. Displacement time history response of the isolation system and the isolated superstructure to the 32.5% 1978 Tabas ground motion

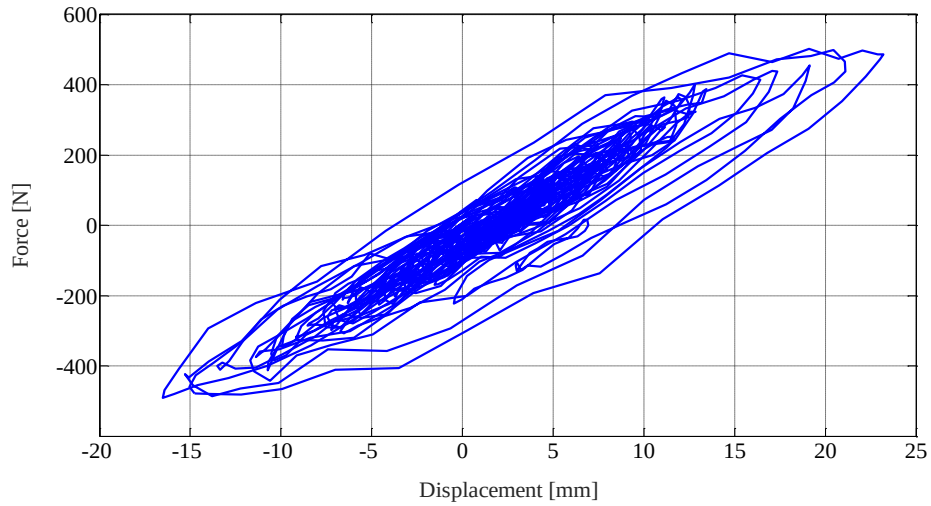

Fig. 6. Force-Displacement response of the isolated superstructure to the 32.5% 1978 Tabas ground motion

3.2.2 Response to the 35% 1971 San Fernando ground motion excitation

The scaled-down San Fernando ground motion acceleration record is shown in Fig. 7.

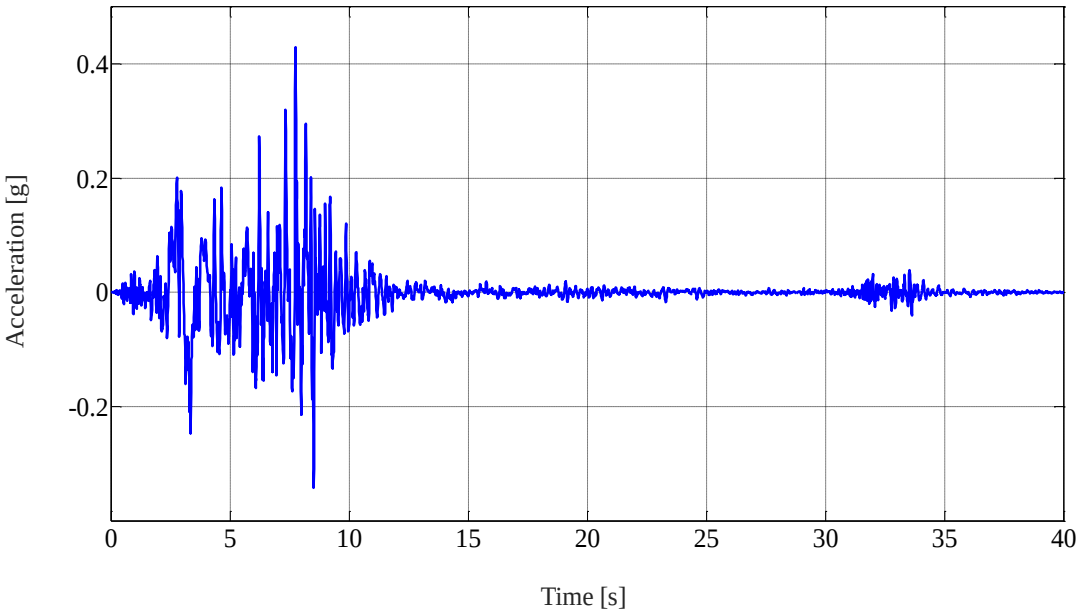

Fig. 7. 35%-scaled 1971 San Fernando ground motion excitation

Fig. 8 shows the measured relative displacement time history of the top mass of the superstructure with respect to the base plate and the relative displacement time history of the base plate with respect to the shaking table.

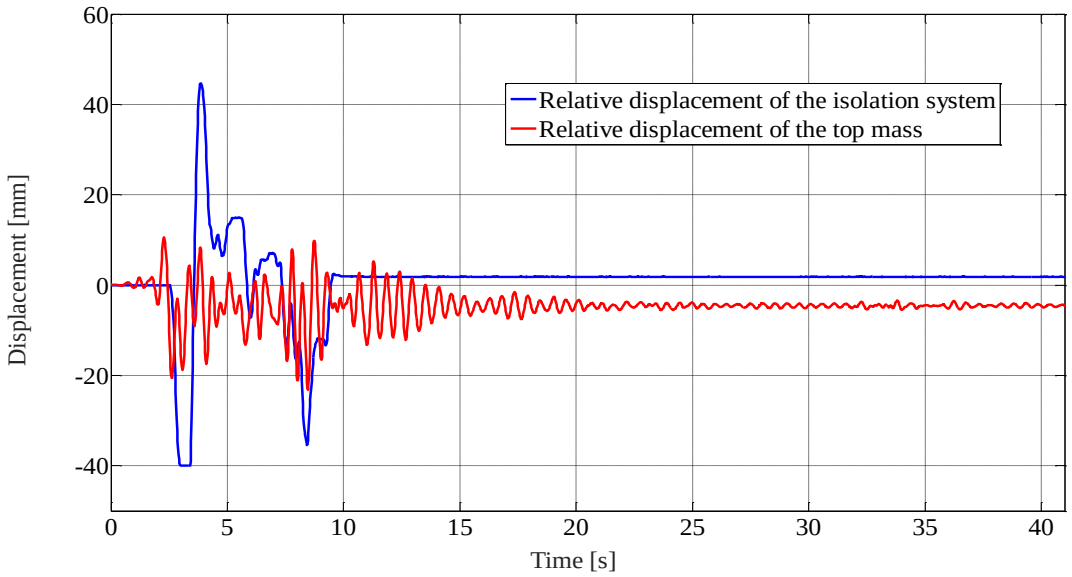

Fig. 8. Displacement time history response of the isolation system and the isolated superstructure to the 35% 1971 San Fernando ground motion

The hysteretic force-displacement loop for the superstructure is presented in Fig. 9. The maximum displacement of the isolation system for this motion was 44.7mm. The maximum displacement of the isolated superstructure with strength reduction factor R_y=1.9 was 23.2 mm. This displacement leads to a displacement ductility ratio μ=1.6.

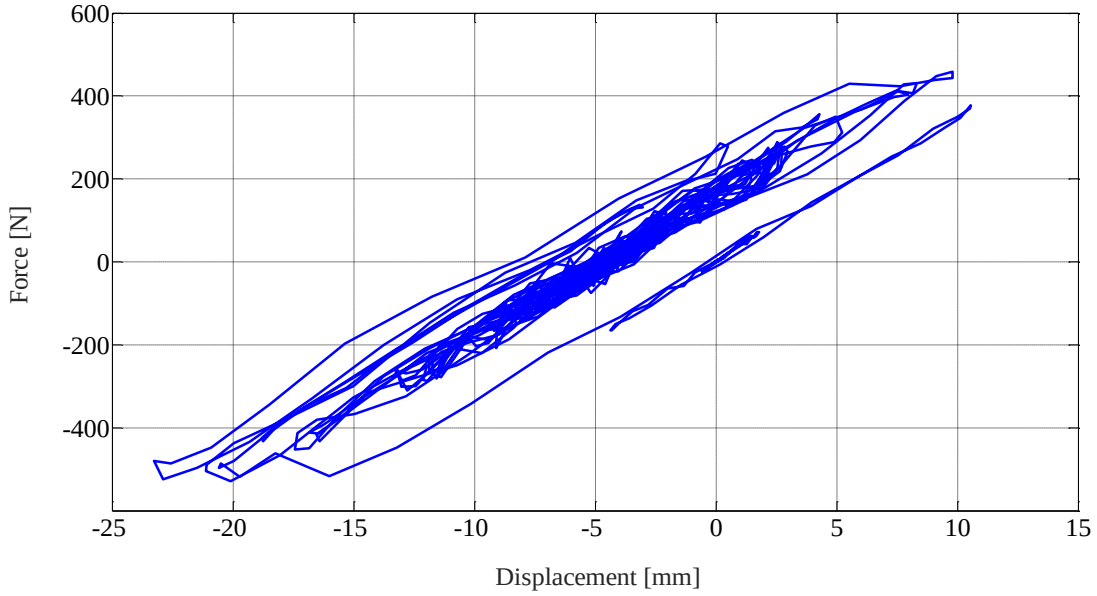

Fig. 9. Force-Displacement response of the superstructure to the 35% 1971 San Fernando ground motion

4. COMPARISON OF THE EXPERIMENTALLY DERIVED RESPONSE WITH THE ANALYTICAL SIMULATION

The comparison of the experimentally derived time history response of the isolation system and the isolated superstructure subjected to Northridge 1994 ground motion excitation with the analytically derived time history response using the model presented in Fig. 1 is shown in Fig. 10 and 11.
The agreement between the displacement time history response of the isolation system that is experimentally determined with the analytically derived response confirms the accuracy of the analytical simulation.

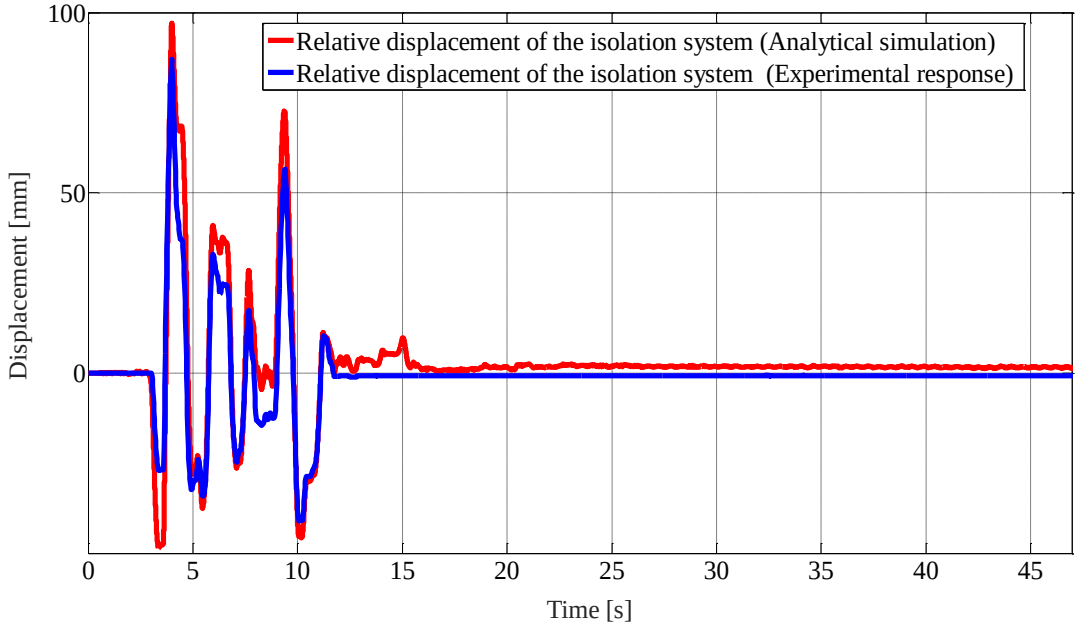

Fig. 10. Response of the specimen with 4 mm, 480 MPa coupons to the 75% 1994 Northridge ground motion excitation: displacement time history responses of the isolation system (analytical simulation and experimental response)

The maximum experimentally derived bearing displacement is 10% lower than the analytically determined value. The high value of static friction (stiction) of the constructed bearings led to the delayed activation of the isolation system compared to the analytically determined activation of the bearings.

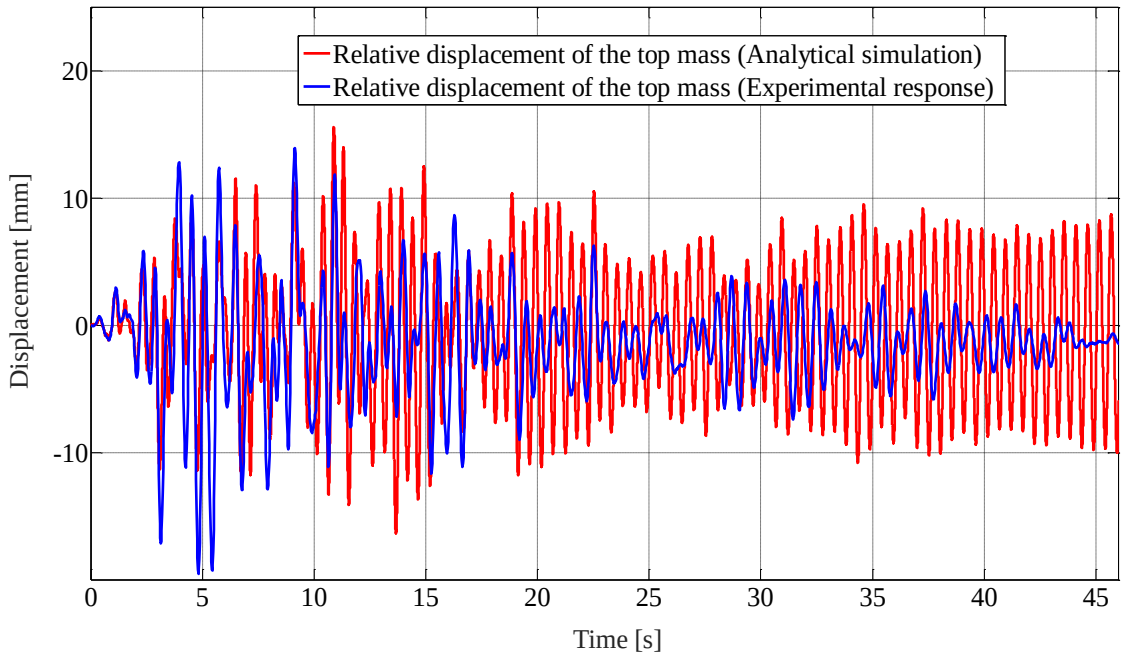

Fig. 11. Response of the specimen with 4 mm, 480 MPa coupons to the 75% 1994 Northridge ground motion excitation: displacement time history responses of the isolated superstructure (analytical simulation and experimental response)

Castaldo et al. (2015) investigated the reliability of structures isolated with friction pendulum bearings and concluded that the use of bearings with lower friction coefficient leads to early activation of the isolation system and better control of the performance of the structure. This delayed activation of the bearings is the main source of difference between the analytically and the experimentally derived response of the isolation system. Lomiento et al. (2013) and Abbiati et al. (2015) concluded that the friction coefficient of sliding bearings can experience changes on the order of −50%, +40%, and −75% due to load, velocity, and cycling effect, respectively.

The experimentally observed displacement time history response of the top mass of the isolated superstructure is similar to the analytically derived response, particularly during the first ten seconds of the motion, when the isolation system gets activated (0-10s). The difference between the experimental response and the analytical simulation of the top mass is attributed to imperfections in the hinge, which resulted in unintended shear deformation of the coupons that cannot be simulated with the cantilever model shown in Fig. 1.

5. STRENGTH-DUCTILITY RELATIONS

The relations between the strength reduction factor R_y, the displacement ductility ratio μ and the vibration period of the structure T_n have been defined by researchers in the past for fixed-base structures using bilinear (Newmark et al. 1973) or trilinear (Vidic et al. 1994) functions. These R_y-μ-T_n relations have been defined by Tsiavos et al. (2017) for base-isolated structures through the analytical investigation of the inelastic response of base-isolated structures subjected to a wide range of ground motion excitations.

The relations between R_y and μ have been determined experimentally in this study for the structure shown in Fig. 2 with a vibration period T_n=0.52s. These relations are compared with the analytically determined R_y-μ-T_n relations for base-isolated structures with γ_m=0.2, the proposed trilinear relations for base-isolated structures with γ_m=0.9 (Tsiavos et al. 2017) and the well-known R_y-μ-T_n relations for fixed-base structures. The results of this comparison are presented schematically in Fig. 12.

As shown in Fig. 12, the experimentally derived R_y-μ-T_n relations are in very good agreement with the analytically derived R_y-μ-T_n relations for γ_m=0.2 for the 1978 Tabas and the 1994 Northridge ground motions. The agreement for the 1971 San Fernando ground motion is not as good; however, the analytically derived R_y-μ-T_n relation is conservative. Similarly, according to the proposed analytical trilinear relations for γ_m=0.9, lower R_y values should be used compared to the experimentally derived values for the same ductility demand μ, thus showing that the proposed relations lead to conservative seismic design and evaluation of inelastic seismically isolated superstructures. On the contrary, the well-known relations for fixed-base structures indicate higher R_y factors for isolated superstructures than the experimentally derived values. Therefore, the existing R_y-μ-T_n relations for fixed-base structures are unconservative and cannot be used for the design and evaluation of base-isolated superstructures. The R_y-μ-T_n relations for base-isolated structures (Tsiavos et al. 2017) should be used for the seismic design and evaluation of seismically isolated superstructures. These R_y-μ-T_n relations indicate that seismically isolated superstructures that enter the inelastic response range will develop displacement ductility demands that exceed the implied strength reduction factor. Therefore, the design code requirement to keep the isolated superstructures in the elastic response range is a sound design strategy.

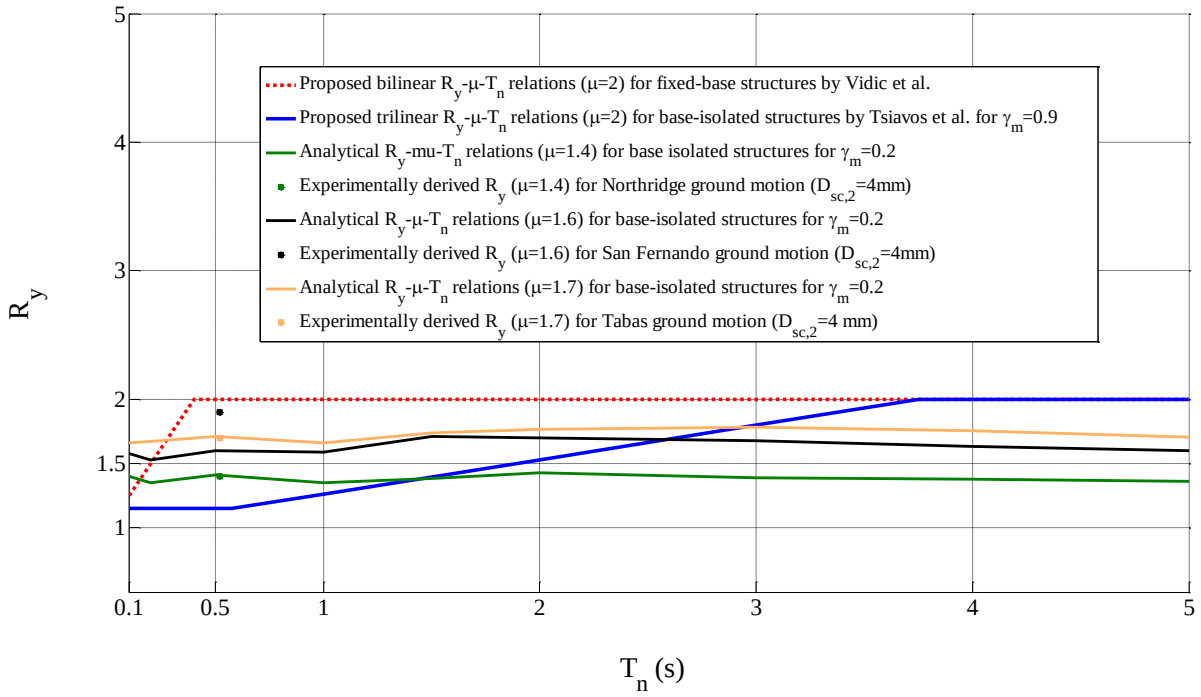

Fig. 12. Comparison of the analytically and experimentally derived R_y-μ-T_n relations

6. CONCLUSIONS

The inelastic behavior of a designed base-isolated structure has been analytically investigated and experimentally verified in this study. The base-isolated superstructure manifested significant inelastic behavior when subjected to the selected ground motion excitations, thus showing that base-isolated structures can develop inelastic behavior due to strong ground motion excitation. This experimentally observed inelastic response of base-isolated structures confirmed the results obtained through the analytical simulation of these structures.

The differences between the experimentally and the analytically derived time history response of the isolation system are related to the high value of stiction of the bearings, which delayed the activation of the isolation system. The existence of an air gap in the hinge has led to unintended shear deformation of

the steel coupons. This shear deformation of the coupons is the main source of the difference between the analytically and experimentally derived time history responses of the isolated superstructure.
The experimentally determined R_y-μ-T_n relations for base-isolated superstructures verify the analytically derived ones proposed by Tsiavos et al. (2017). The R_y-μ-T_n relations for fixed-base structures are unconservative for base-isolated superstructures and cannot be used neither for the seismic design nor for the seismic evaluation of these superstructures. The relations proposed by Tsiavos et al. (2017) should be used instead.

7. REFERENCES

Constantinou MC, Mokha A, Reinhorn A (1990) Teflon bearings in base isolation. II: Modeling. *Journal of Structural Engineering* (ASCE). 116 (2): 455–474.

Becker TC, Mahin SA (2012). Experimental and analytical study of the bi-directional behavior of the triple friction pendulum isolator. *Earthquake Engineering and Structural Dynamics*, 41(3):355–373.

Lignos DG (2012). Modeling and experimental validation of a full scale 5-story steel building equipped with triple friction pendulum bearings: E-defense blind analysis competition. *In Proc., 9th Int. Conf. on Urban Earthquake Engineering (9CUEE) and 4th Asia Conf. on Earthquake Engineering*, Center for Urban Earthquake Engineering (CUEE).

Shi Y, Kurata M, Nakashima M (2014). Disorder and damage of base-isolated medical facilities when subjected to near-fault and long-period ground motions. *Earthquake Engineering and Structural Dynamics*, 43 (11):1683–1701.

Constantinou MC, Quarshie JK (1998). Response modification factors for seismically isolated bridges. *Report No. MCEER-98-0014*, Center for Earthquake Engineering Research, Buffalo, NY.

Whittaker AS, Sollogoub P, and Kim MK (2017). Seismic isolation of nuclear structures: past, present and future, *24th Conference on Structural Mechanics in Reactor Technology BEXCO, Busan, Korea - August 20-25*.

Sollogoub P (1994). Inelastic behavior of structures on aseismic isolation pads, *Tenth European Conference on Earthquake Engineering*, Vienna, Austria.

Kikuchi M, Black CJ, Aiken ID (2008). On the response of yielding seismically isolated structures. *Earthquake Engineering and Structural Dynamics*, 37(5):659–679.

Thiravechyan P, Kasai K, Morgan TA (2012). The effects of superstructural yielding on the seismic response of base-isolated structures, *Joint Conference proceedings, 9th International Conference on Urban Earthquake Engineering / 4th Asia Conference on Earthquake Engineering*, Tokyo, Japan, 1451-1458.

Cardone D, Flora A, Gesualdi G (2013). Inelastic response of RC frame buildings with seismic isolation. *Earthquake Engineering and Structural Dynamics*, 42:871–889.

Tsiavos A, Mackie KR, Vassiliou MF and Stojadinovic B (2017). Dynamics of inelastic base- isolated structures subjected to recorded ground motions. *Bulletin of Earthquake Engineering*, **15**(4):1807–1830.

Tsiavos A, Vassiliou MF, Mackie KR and Stojadinovic B (2013a). R-μ-T relationships for seismically isolated structures, COMPDYN, *4th International Conference on Computational Methods in Structural Dynamics and Earthquake Engineering*, Kos Island, Greece, 12-14 June.

Tsiavos A, Vassiliou MF, Mackie KR and Stojadinovic B (2013b). Comparison of the inelastic response of base-isolated structures to near-fault and far-fault ground motions, *VEESD, Vienna Congress on Recent Advances in Earthquake Engineering and Structural Dynamics & D-A-CH Tagung*, Vienna, Austria, 28-30 August.

Vassiliou MF, Tsiavos A and Stojadinovic B (2013). Dynamics of inelastic base-isolated structures subjected to analytical pulse ground motions, *Earthquake Engineering and Structural Dynamics*, 42 (14), 2043-2060.

Kelly JM (1997), Earthquake Resistant Design with Rubber. Springer: London.

Katsanos EI, Sextos AG (2015). Inelastic spectra to predict period elongation of structures under earthquake loading. *Earthquake Engineering and Structural Dynamics*, 44(11):1765–1782.

Mavronicola E, Komodromos P (2014). On the response of base-isolated buildings using bilinear models for LRBs subjected to pulse-like ground motions: sharp vs. smooth behaviour. *Earthquake Structures,* 7(6):1223–1240.

PEER NGA strong motion database (2010). Pacific Earthquake Engineering Research Center, Berkeley, California (http://peer.berkeley.edu/nga/ on 08.09.2014).

Castaldo P, Palazzo B, Della Vecchia P (2015). Seismic reliability of base-isolated structures with friction pendulum bearings, *Engineering Structures*, 95, 80-93.

Lomiento G, Bonessio N, Benzoni G (2013). Friction model for sliding bearings under seismic excitation, *Journal of Earthquake Engineering*, 17(8):1162–1191.

Abbiati G, Bursi OS, Caperan P, Di Sarno L, Molina FJ, Paolacci F, Pegon P (2015). Hybrid simulation of a multi-span RC viaduct with plain bars and sliding bearings. *Earthquake Engineering and Structural Dynamics*, 44:2221– 2240.

Vidic T, Fajfar P, Fischinger M (1994). Consistent inelastic design spectra: strength and displacement. *Earthquake Engineering and Structural Dynamics*, 23, 502–521.

Newmark NM, Hall WJ (1973), Seismic design criteria for nuclear reactor facilities, *Report 46*, Building Practices for Disaster Mitigation, National Bureau of Standards, 209–236.